PHASE IDENTIFICATION IN TWIN-ROLL CAST Al-Li ALLOYS

[1]Lucia BAJTOŠOVÁ, [2]Olexandr GRYDIN, [2]Mykhailo STOLBCHENKO, [2]Mirko SCHAPER, [1]Barbora KŘIVSKÁ, [1]Rostislav KRÁLÍK, [1]Michaela ŠLAPÁKOVÁ, [1]Miroslav CIESLAR

[1]Charles University, Faculty of Mathematics and Physics, Praha, Czech Republic, EU,
lucibajtos@gmail.com, krivska.barbora@seznam.cz, rkralik96@gmail.com, slapakova@karlov.mff.cuni.cz, cieslar@met.mff.cuni.cz

[2]Paderborn University, Chair of Materials Science, Paderborn, Germany, EU,
grydin@lwk.upb.de, stolbchenko@lwk.upb.de, schaper@lwk.upb.de

https://doi.org/10.37904/metal.2022.4437

Abstract

Al-Li-based alloys are an attractive material for aircraft and aerospace applications. Preparation of these alloys by twin-roll casting (TRC), which combines rapid metal solidification and subsequent plastic reduction in a single processing step, could improve the properties of the alloys compared to materials prepared by conventional direct-chill casting. A commonly used approach for identifying primary phases is a chemical analysis by energy dispersive spectroscopy (EDS). More accurate results can be achieved by combining the method with diffraction analysis. This process can be considerably simplified in microscopes equipped with automated crystal orientation and phase mapping (ACOM-TEM). Al-Cu-Li-Mg-Zr alloy was prepared by twin-roll casting. A combination of TEM and STEM images with chemical analysis by EDS and ACOM-TEM was used to obtain complex information about phases of boundary primary particles. The efficiency of the individual methods for the phase identification in TRC Al-Li-based alloys is discussed.

Keywords: Al-Cu-Li-M-Zr-Fe alloy, twin-roll casting, phase identification, ACOM-TEM

1. INTRODUCTION

The wide use of aluminum-lithium alloys in the aircraft and aerospace industry is conditioned by its advantageous properties, particularly low density, high stiffness, and high strength [1-3]. These properties result from the addition of lithium to aluminum alloys, as the addition of 1 wt.% of lithium causes the density of Al alloys to decrease by 3%, their Young modulus to increase by 6%, and allows a formation of hardening precipitates [4,5]. An effort to further improve the mechanical and corrosion properties led to optimizing the composition of alloying additions. Adding Mg and Cu has been shown to produce additional strengthening Cu- and Mg- phases and alter the solubility of the most important alloying elements, thus improving the precipitation [6,7]. The following precipitates could contribute to the strengthening: δ'(Al_3Li), θ'(Al_2Cu), T1(Al_2CuLi), S' (Al_2CuMg), and T2(Al_6CuLi_3). For alloys with Li content lower than 1.5 wt%, the formation of metastable δ'(Al_3Li) is suppressed, and the strengthening is mainly achieved through θ', T1, and S' phases [8]. Overaging results in the formation of coarse T(Al_2MgLi) and S(Al_2CuMg) phases near grain boundaries [6]. The balance of the θ', T1 and S' phases depends on the relative concentrations of the three additions. The addition of Zr leads to the precipitation of Al_3Zr metastable particles, which could further support the strengthening and thermal stabilization of the microstructure [9]. Apart from the precipitate phases, coarse primary phases (S (Al_2CuMg), θ(Al_2Cu), S(Al_2CuMg), and Li-rich T phases) and impurities (like Fe and Si) coarse particles could form at grain boundaries, which can negatively affect the properties of the alloy [10]. They should be dissolved or transformed during a homogenization treatment. Twin roll casting of Al-Li-based alloys could provide a favorable alternative to the commonly used direct chill (DC) casting. Grains and boundary particles of primary phases formed during the TRC process are usually finer than the ones in DC cast alloys. Therefor lower

annealing temperatures and shorter soaking times are required during the homogenization of TRC alloys [11,12]. Optimizing the homogenization treatment requires reliable and statistically relevant information about the phase composition and distribution of primary phase particles. Energy dispersive spectroscopy (EDS) provides a quick way to distinguish Cu- or Fe- based phases. However, no information about Li could be gained. Any reliable determination of the phase type moreover requires a time-consuming analysis of diffraction patterns. This process could be significantly accelerated in modern microscopes equipped with automated crystal orientation and phase mapping (ACOM-TEM) option [13]. ACOM-TEM could also be used in studies performed on specimens annealed in-situ in TEM because, unlike EDS, it is not disturbed by parasitic infrared radiation at elevated temperatures simulating the behavior of the alloy during a high-temperature homogenization treatment

In the present work, the potential of ACOM-TEM for identifying primary phases in TRC Al-Cu-Li-Mg-Zr-Fe alloy was tested, and the results of the method were compared with results received by EDS chemical analysis and examination of selected area diffraction patterns.

2. EXPERIMENTAL METHODS

Al-Cu-Li-Mg-Zr-Fe alloy of a third-generation with composition given in **Table 1** was used as the input material for the twin-roll casting.

Table 1 Chemical composition of Al-Cu-Li-Mg-Zr-Fe alloy in wt%

Al	Cu	Li	Mg	Zr	Fe
balance	3.71	0.91	0.31	0.15	0.05

The 3 mm thick strips were produced using the laboratory twin-roll caster of the Paderborn University. A detailed description of the twin-roll caster can be found in [14]. The specimens for the TEM were electropolished in 30% HNO_3 solution in methanol at temperatures near −20 °C.

TEM bright field (BF) and diffraction images, STEM BF and HAADF images, and ACOM-TEM orientation maps were taken by JEOL JEM 2200 FS operating at an accelerating voltage of 200 kV. The microscope was equipped with the “Spinning Star” electron precession from NanoMEGAS with an ASTAR software package and JEOL Centurio EDS detector.

3. RESULTS AND DISCUSSION

Several primary phase particles of each different type were analyzed. Examples of STEM images are shown in **Figures 1, 2 a)**. Elemental maps confirm the presence of Cu and Mg in the whole length of the first particle (**Figure 1**). The presence of Al in the map is shaded by a strong signal from the surrounding Al matrix, with the thickness decreasing at the boundary. Small areas of higher Fe content originated from small Fe-rich particles embedded in the observed boundary phase. Quantification of the results is affected by the surrounding Al grains. However, since only three elements are significant and the amount of Cu and Mg is approximately the same, the phase of the particle is most probably equilibrium S (Al_2CuMg), an orthorhombic phase with lattice parameters: a = 0.40119 nm, b = 0.9265 nm and c = 0.7124 nm [15].

A similar approach was applied to the second particle (**Figure 2**). Elemental maps show an increased amount of Cu and Fe in the particle, the amount of Al is again shadowed by the matrix, map of Mg does not exhibit increased concentration in the particle. Quantifying the signal from a part of the particle evidences that the amounts of Mg and Fe are under 4 at%, while concentrations of Al and Cu are almost 50 at% each. This suggests that the particle is probably monoclinic AlCu phase [16]. The presence of Zr was not detected in any of the studied boundary particles, most probably due to a relatively low nominal Zr concentration, high solidification rate during TRC, and a peritectic feature of the Al-Zr system at low Zr concentrations [17]. Since

the precipitation of Al_3Zr metastable particles was shown not to occur before annealing at high temperatures (above 500 °C) for an extended time [14], it can be concluded that the Zr is fully dissolved in the Al matrix.

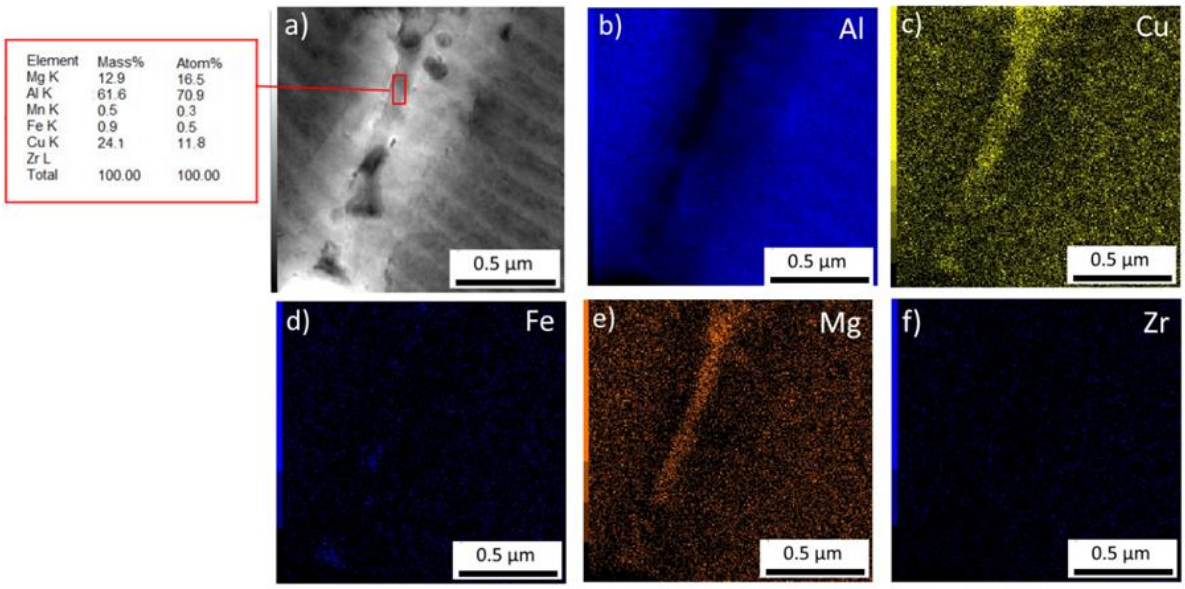

Figure 1 a) STEM image of a boundary particle and its EDS quantification, b-f) EDS element maps.

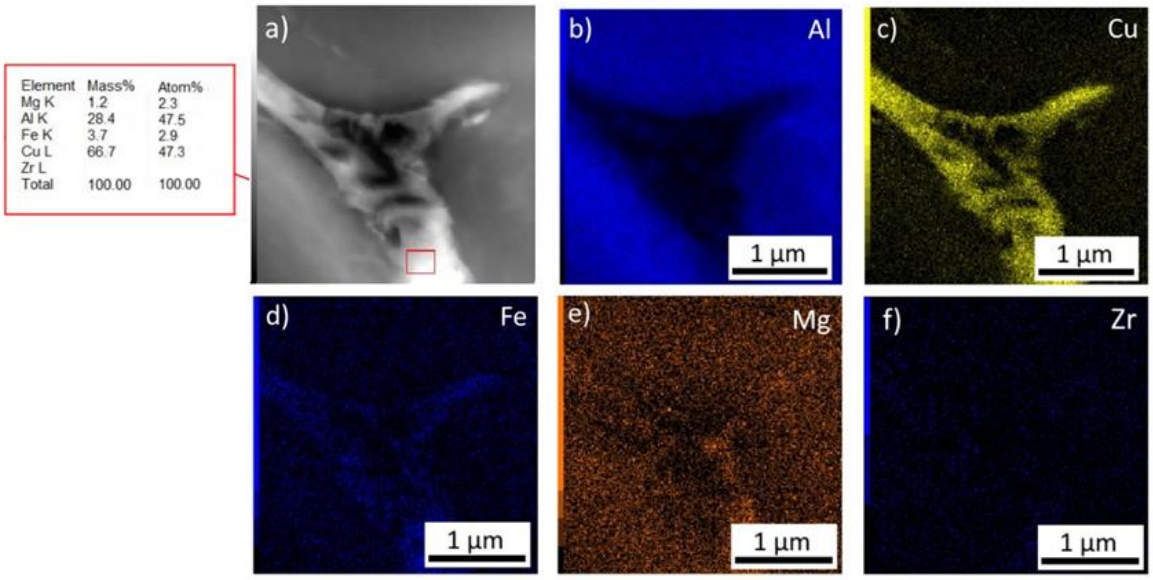

Figure 2 a) STEM image of a boundary particle and its EDS quantification, b-e) EDS element maps.

Diffraction patterns of both particles were then analyzed via ASTAR automatic phase and orientation mapping (**Figures 3** and **4**).

The pattern of the particle from **Figure 1** (**Figure 3**) was identified with a high probability as S (Al_2CuMg) phase with a satisfactory match between the generated and experimental pattern (**Figure 3b,c**). The results agree with the results obtained by the EDS analysis, as it is also confirmed by a high Astar image index for the S (Al_2CuMg) phase (**Figure 3d**). Orientation maps of the S-phase are shown in **Figure 3e-g)**. Results from the orientation and phase matching for the particle from **Figure 2a)** are shown in **Figure 4**.

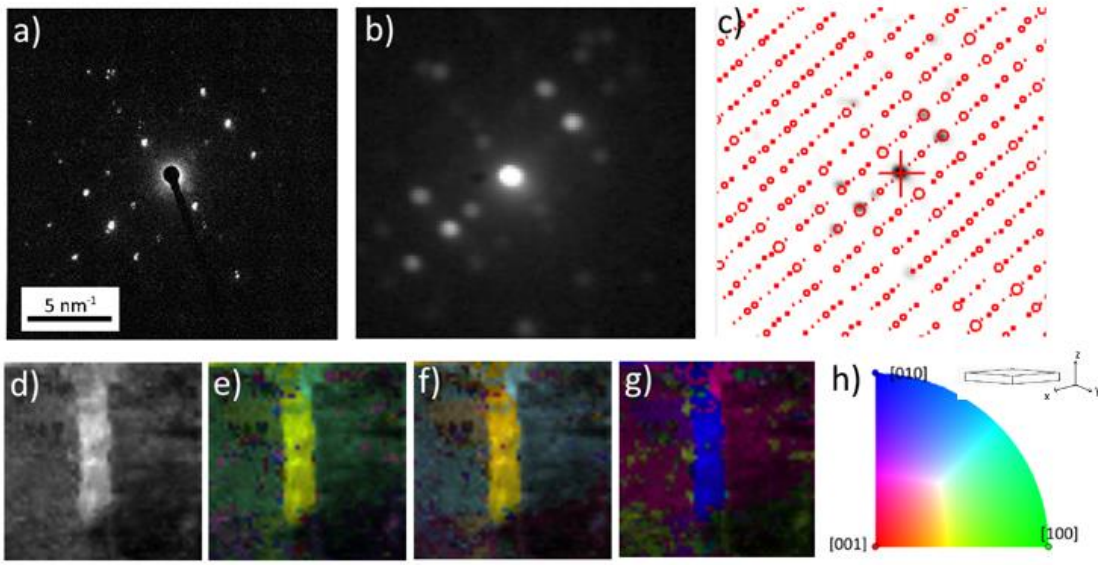

Figure 3 Diffraction patterns and corresponding orientation maps obtained from the particle shown in **Figure 1**, a) SAED diffraction pattern, b) ASTAR diffraction image, c) ASTAR match to S (Al_2CuMg) template, d) ASTAR index image, e-g) ASTAR orientation maps, h) S (Al_2CuMg) orientation triangle.

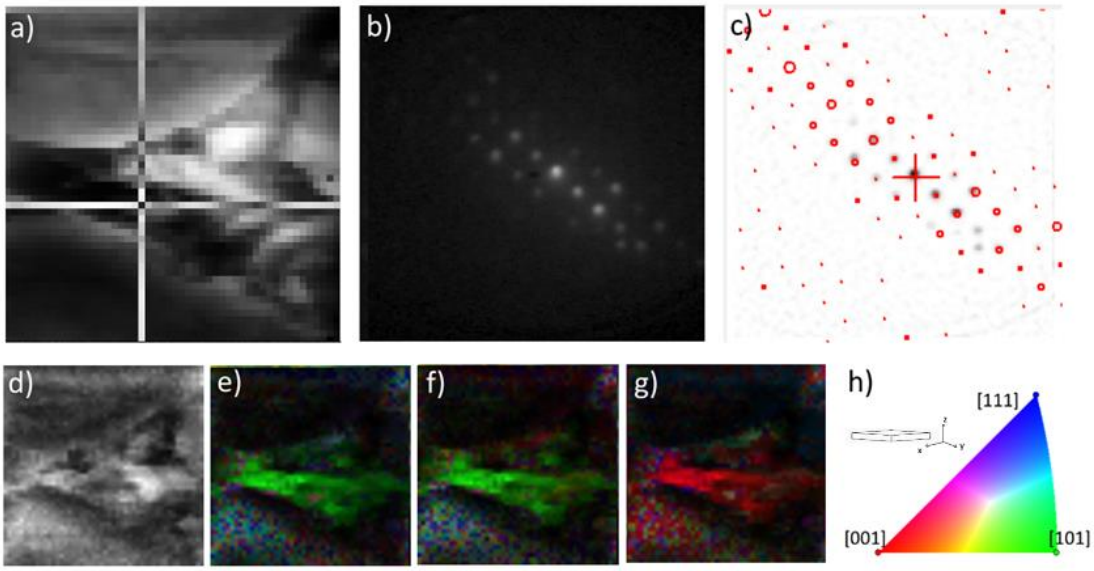

Figure 4 ASTAR images of the particle in **Figure 2**, a) virtual BF, b) diffraction image, c) match to Al_2Cu template, d) index image, e-g) orientation maps, h) Al_2Cu orientation triangle.

The most probable match was obtained for the θ(Al_2Cu) [18] phase. Index and orientation maps for Al_2Cu (**Figure 4d-g**) show good correspondence in the lower part of the particle. The problem with identifying the upper part is connected to the slightly different orientation of the particle with a lower number of diffraction spots and their overlap with the diffraction pattern on the surrounding Al matrix. The result contradicts the finding following from the EDS analysis, which identified the phase as the AlCu phase. Inaccuracy in the quantification follows most probably from the absorption of the Al EDS signal in the particle [19].

Figure 5 shows an example of an Al_2CuLi phase boundary particle found and identified by ACOM-TEM. This type of phase appears relatively rarely inside the TRC material. Nevertheless, in contrast to the EDS analysis (EDS could not detect Li), this phase could be identified by the ASTAR software, proving thus the enhanced

analytical efficiency of the method. ACOM-TEM could quickly identify a majority of primary phases containing main constituent elements. However, it fails in the case when the particle is embedded in the matrix or another phase.

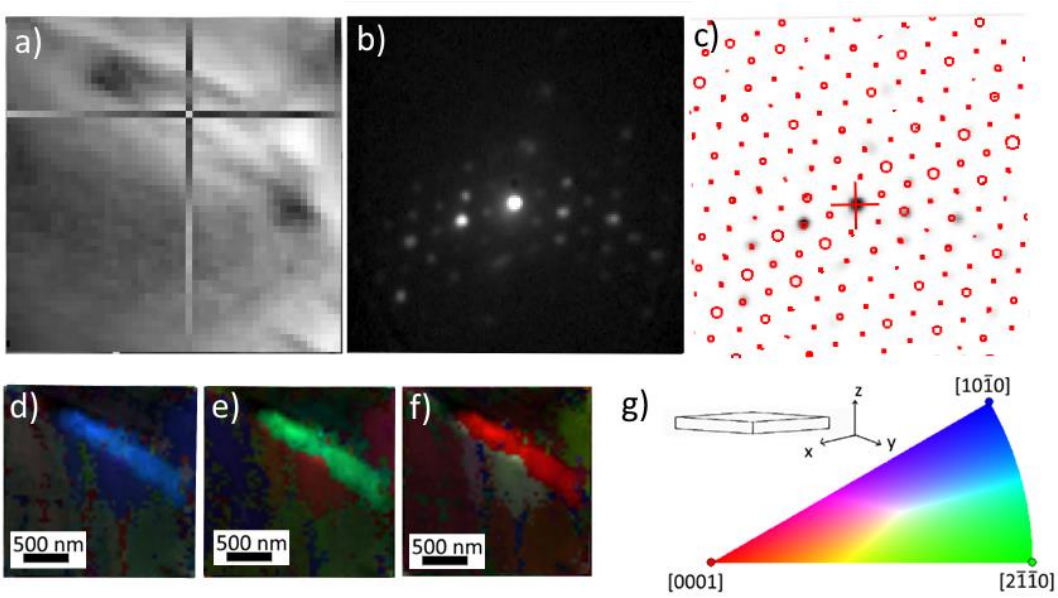

Figure 5 Diffraction ASTAR analysis of a boundary particle a) virtual BF, b) diffraction image, c) simulated diffraction pattern of Al_2CuLi, d-f) ASTAR orientation maps, g) Al_2CuLi orientation triangle.

4. CONCLUSION

The phases of the coarse boundary particles in a TRC Al-Li-based alloy were identified via energy dispersive spectroscopy and automated orientation mapping in TEM. ACOM-TEM could easily identify phases containing lithium, a result that EDS could not receive. However, the results are affected by the thickness of the particles, their local orientation changes, and the surrounding matrix. More than one systematic line of diffraction spots is necessary for a credible phase identification via automated mapping. The ACOM-TEM technique could be promising for evaluating phase changes in situ at elevated temperatures. The presence of Al_2Cu, Al_2CuLi, and Al_2CuMg phases was confirmed.

ACKNOWLEDGEMENTS

The authors would like to thank the Czech Science Foundation project number 20-19170S and the German Research Foundation (Deutsche Forschungsgemeinschaft (DFG)) for financial support within the scope of project SCHA 1484/46-1.

REFERENCES

[1] PRASAD, Namburi Eswara, et al. Mechanical behavior of aluminium-lithium alloys. *Sadhana*. 2003, vol. 28, pp. 209–246.

[2] FERRY, Michael M. *Direct strip casting of metals and alloys – Processing. Microstructure and properties*. Cambridge: Woodhead Publishing Ltd. 2006, pp. 101–194.

[3] STARKE, Edgar A., STALEY, James T. Application of modern aluminum alloys to aircraft. *Progress in Aerospace Sciences.* 1996, vol. 32, pp. 131-172.

[4] ABD EL-ATY, Ali, NAMBURI Eswara, et al. Experimental investigation of tensile properties and anisotropy of 1420, 8090 and 2060 Al-Li alloys sheet undergoing different strain rates and fibre orientation: A comparative study. *Procedia Engineering*. 2003, vol. 207, pp. 13-18.

[5] LAVERNIA, Enrique J. et al. Strength, deformation, fracture behavior and ductility of aluminium-lithium alloys. *The Journal of Materials Science*. 1990, vol. 25, pp. 1137–1158.

[6] PRASAD, Konduri Sartye et al. *Aluminum-lithium alloys processing properties and applications*. Butterworth-Heinemann. Imprint of Elsevier, 2014, pp. 99-137.

[7] RIOJA, Roberto J., LIU, John. The evolution of Al-Li based products for aerospace and space applications. *Metallurgical and Materials Transactions A*. 2012, vol. 43, pp. 3325–3337.

[8] DORIN, Thomas, et al. *Aluminium lithium alloys in book Fundamentals of aluminum metallurgy*. Elsevier, 2010, pp. 387-438.

[9] MARQUIS, Emmanuelle A., SEIDMAN, David N. Nanoscale structural evolution of Al3Sc precipitates in Al(Sc) alloys. *Acta Materialia*. 2001, vol. 49, pp. 1909–1919.

[10] MA, Yanlong, et al. Distribution of intermetallics in an AA 2099-T8 aluminum alloy extrusion. *Materials Chemistry and Physics*. 2011, vol. 126 no. 1, pp. 46–53.

[11] BAREKAR, Nilam S., DHINDAW, Brij K. Twin-roll casting of aluminum alloys. An overview*. Materials and Manufacturing Processes*. 2014, vol. 29, pp. 651–661.

[12] BERG, Bjørn S. et al. Gauge reduction in twin-roll casting of an AA5052 aluminum alloy: the effects on microstructure. *Journal of Materials Processing Technology.* 1995, vol. 53, pp. 65–74.

[13] RAUCH, Edgar F., VERON, Muriel. Automated crystal orientation and phase mapping in TEM. *Materials Characterization.* 2014, vol. 98, pp. 1–9.

[14] GRYDIN, Olexander, et al. New twin-roll cast Al-Li based alloys for high-strength applications. *Metals*. 2020, vol. 10, pp. 987.

[15] HEYING, Birgit et al. Structure refinement of the S-phase precipitate $MgCuAl_2$. *Zeitschrift für Naturforschung B*. 2005, vol. 60, pp. 491 – 494.

[16] PONWEISER, Norbert, et al. Re-investigation of phase equilibria in the system Al-Cu and structural analysis of the high-temperature phase η1-Al1-δCu. *Intermetallics*. 2011, vol. 19, pp. 1737-1746.

[17] JANGHORBAN, Amin, et al. Phase equilibria in the aluminium-rich side of the Al–Zr system. *Journal of Thermal Analysis and Calorimetry*. 2013, vol. 114, no. 3, pp. 1015–1020.

[18] MEETSMA, Auke M. et al. Refinement of the crystal structure of tetragonal Al2Cu. *Journal of Solid State Chemistry*. 1989, vol. 83, pp. 370-372.

[19] RUSS, John C. *Chapter 6 - X-Ray Absorption, Fundamentals of Energy Dispersive X-ray Analysis*. Butterworth-Heinemann, 1984, pp. 69-80.